International Journal on Advanced Science Engineering Information Technology

Vol.14 (2024) No. 3
ISSN: 2088-5334

Partial Least Square Regression for Nondestructive Determination of Sucrose Content of Healthy and *Fusarium spp*. Infected Potato (*Solanum tuberosum L.*) Utilizing Visible and Near-Infrared Spectroscopy

Eko Widi Prasetyo [a], Hanim Zuhrotul Amanah [a], Ibnu Farras [a], Muhammad Fahri Reza Pahlawan [b], Rudiati Evi Masithoh [a,*]

[a] *Department of Agricultural and Biosystems Engineering, Faculty of Agricultural Technology, Universitas Gadjah Mada, Yogyakarta, Indonesia*
[b] *College of Agriculture and Life Science, Department of Biosystems Machinery Engineering, Chungnam National University, Yuseong-Gu Daejeon, Republic of Korea*

Corresponding author's : [*]evi@ugm.ac.id

Abstract*—Conventional methods of quantifying the chemical content of potatoes at different storage temperatures are time-consuming and expensive. This research studied the Visible and Near Infrared (Vis-NIR) spectroscopy for possible rapid and nondestructive methods. In this study, healthy and *Fusarium spp.* Potato seeds of Granola L varieties were infected artificially through the process of inoculation of fungi, and healthy potatoes were stored in various post-harvest storage conditions, namely temperatures 12°C, 25°C and a combination of temperatures 12°C and 25°C. VIS-NIR spectral data from seeds are observed periodically during the storage period. The study results showed that Vis-NIR predicted sucrose content in potatoes. The best-developed PLSR calibration model for potatoes stored at 25°C and a combination of 12°C and 25°C show R2c of 0.87 and 0.83 and RMSEC of 0.26 and 0.28. The models also successfully predicted the sugar content of potato stored at 25°C and a combination of temperatures 12°C and 25°C with R^2p 0.75 and 0.78, RMSEP of 0.36 and 0.32, and RPD of 1.99 and 2.81 for sucrose. The developed model of sucrose content or potato storage temperatures of 12°C is not recommended for monitoring and detection due to the low RPD < 1.9 even though the R^2c values are 0.65 – 0.9. the results of this investigation indicate that VIS-NIR spectroscopy could potentially serve as a tool for quantifying the chemical composition of potatoes during post-harvest storage.

***Keywords*—Visible and near-infrared; spectroscopy; potato; PLSR; Fusarium spp.**

Manuscript received 28 Dec. 2023; revised 12 Mar. 2024; accepted 3 Apr. 2024. Date of publication 30 Jun. 2024.

I. INTRODUCTION

Potato (*Solanum tuberosum L.*) holds significant prominence as one of the most extensively cultivated crops globally. It serves as a fundamental dietary component in numerous developed and developing nations, contributing to its status as a staple food. Potatoes are ingested in their uncooked state as a fundamental sustenance or vegetable, transformed into French fries, crisps, and additional culinary enhancements, and employed in the production of potato flour, starch, and alcohol [1]. According to the data provided by the Food and Agriculture Organization *(FAO)*, the global production of potatoes amounted to a significant quantity of 376 million metric tons. In 2021, China and India emerged as the leading nations in potato production, with 94 million metric tons and 54 million metric tons, respectively (FAO, 2022). The escalating need resulting from the expanding populace and processing sectors has engendered a substantial impetus for augmented output. Concurrently, mitigating detriments inflicted by biotic and abiotic pressures is paramount in cultivating potatoes.

Potatoes are susceptible to numerous pathogens that can result in substantial direct or indirect losses in their production. Because potatoes are underground vegetable crops that reproduce asexually, the risk of soil- and tuber-borne illnesses is always present. [3]. Furthermore, fungal pathogens, among other biotic stresses, pose a significant constraint in the potato production system and can lead to economic losses in the field and during transportation and storage [4]. In particular, the sugar content, namely sucrose,

glucose, and fructose, is a vital determinant of the intrinsic quality of potatoes [5]. This determinant directly correlates to the vegetable's nutritional worth, taste, and durability [6], [7]. Sucrose or non-reducing sugar is one of the disaccharide compounds with a chemical systematics called α-D-gluco-pyranosyl-β-D-fructofuranoside and molecular formula C12H22O11 [4]. Sucrose levels in potatoes can be used to assess ripeness (such as harvest age) and fungal damage (such as *Fusarium spp.* infection) [8], [9].

Detecting internal defects in potatoes, such as internal brown spots, hollow heart, heat necrosis, and black heart, poses a significant challenge for food engineering. The most conventional approaches employed to assess the internal quality of potatoes are characterized by their destructive nature and inefficiency [10]. These internal defects are not readily apparent until the tubers are cut or peeled, leading to economic losses in the potato industry. Growers cannot distinguish between healthy and defective potatoes, resulting in waste during processing and undermining consumer confidence. A practical assessment system in potato production should possess notable attributes such as accuracy, rapidity, and cost-effectiveness.

Those issues can be addressed using nondestructive techniques, which can potentially separate raw potato tubers based on the presence of internal defects before they are brought to the fresh market or processed. Several noninvasive methodologies, such as spectroscopic techniques, computer vision systems, and ultrasound methods, have been extensively examined to evaluate internal defects in potato tubers. However, the efficacy of these techniques varies depending on the specific type of defect [11], [12].

According to Nieto-Ortega et al., reflectance spectroscopy has appeared as an up-and-coming technique for agricultural management owing to its nondestructive, expeditious, and comparatively cost-effective characteristics in the monitoring of vegetation conditions [13]. The success of reflectance spectroscopy for studying plants relies on the relationship between light and their chemical and structural makeup and water content. The reflection of light across the visible spectrum (400 to 700 nm), near-infrared spectrum (NIR, 700 to 1,100 nm), and shortwave infrared spectrum (SWIR, 1,100 to 2,400 nm) allows for a holistic evaluation of changes in visual indicators such as pigments and leaf color, as well as the underlying biochemical factors such as nutrient composition and secondary metabolism, and physiological responses such as photosynthetic activity and water relations, in response to disease or stress [14], [15].

II. Materials and Methods

A. Sample Preparation

One hundred and sixty-five potato tubers of cultivar *Granola L.* were obtained from the same source in the Research Field of PT. BISI International, Tbk., located in Pujon, Malang, East Java, Indonesia. The planting occurred 1109 meters above sea level, with average daily temperatures ranging from 20 to 30°C. The potato tubers were harvested from August to September 2022. The collected samples were ensured to be freshly harvested and free from fungal spores, pests, and diseases before their transfer to the Biophysics Engineering Laboratory, Faculty of Agriculture Technology, Universitas Gadjah Mada, for subsequent examination.

One hundred and sixty-five potato tubers (165), with an average weight of 30 g and uniform size, underwent a thorough cleansing process using tap water to eliminate any traces of soil. The tubers were dried before analysis, sterilized with a 1% NaClO solution (sodium hypochlorite) for 10 minutes, rinsed with distilled water, and dried again. Standard cuts of 30 mm × 30 mm were made on all tubers using sterile electric drills. The fungal pathogen used in this study was *Fusarium spp.*, prepared using the cork borer wounding (CBW) method described by Farokhzad et al. [16]. This process involved utilizing 500 g of commercially available *Fusarium solani* inoculant powder containing spores or other fungal propagules suitable for application. However, the fungal pathogen in the present study was isolated from artificially infected potato tubers, not directly from the inoculant powder. The pathogen isolation procedure was carried out on tubers exhibiting symptoms of dry rot. In a laminar cabinet, 1 mm x 1 mm sections of diseased and healthy tissue were excised from the infected tubers. These sections were then subjected to surface sterilization using a sequential process: 1% sodium hypochlorite for 1 minute, followed by 70% ethanol for 30 seconds, and finally washed with distilled water. Subsequently, the sterilized tissue pieces were placed on potato dextrose agar (PDA) media and incubated at a temperature range of 18 °C to 24 °C. Following a two-day incubation period, the initial fungal growth observed only on the diseased tissue was meticulously transferred to fresh PDA plates to establish a pure fungal culture. One hundred and ten samples (110) were randomly selected for artificial infection with *Fusarium spp.* inoculum. The inoculum was applied to the uniform lesions on each tuber, which the electric drills had created. The remaining fifty-five (55) samples were kept without infections as the control group.

Potato tubers were stored in plastic containers in dark storage for 30 days. The inside of each container has a layer of damp filter paper at the bottom, and then the plastic container is closed. The samples were treated as shown in Table 1. Relative humidity was maintained at 85% for all variations. Meanwhile, the Testo 174H Data Logger combines and stores temperature and humidity (RH) data. Data observation was taken every five days.

TABLE I
SAMPLE CODES AND TREATMENT USED IN THIS RESEARCH

Samples	Treatment
T12°C	Stored at 12ºC temperature for 30 days
T25°C	Stored at 25ºC temperature for 30 days
T12ºC25ºC	Stored at 12ºC temperature for 10 days, followed by storing at 25ºC for 20 days

B. Spectra Measurement

Spectral measurement of potato tubers is carried out using two types of modular spectrometers: Vis-NIR Miniature Spectrometer and NIR Miniature Spectrometer (Figure 1). The instrument used in this study consists of 4 components, namely Vis-NIR Miniature Spectrometer (Type: Flame-T-VIS-NIR Ocean Optics, Wavelength range: 350-1000 nm, optical resolution: ~0.1-10.0 nm FWHM), NIR Miniature Spectrometer (Type: FLAME-NIR+ Ocean Optics,

Wavelength range: 1000-1600 nm, Optical resolution: 10.00 nm FWHM), high-powered halogen tungsten lamp (Type: HL-2000-HP-FHSA Ocean Optics, wavelength range: 360-2400 nm, Fiber Connector SMA 905, nominal bulb power 20 W, typical output power 8.4 mW), and Fiber optic cable reflection probe (Type: QR400-7-VIS-NIR Ocean Optics, wavelength range: 400-2100nm).

The reflectance standard (Type: WS-1 Diffuse Reflectance Standard, Material: PTFE) was used for calibration. The process of obtaining spectra involves conducting spectra capture settings. Ocean View 2.0.12 software collected reflectance spectra in the Vis-NIR and SW-NIR regions. Distance from probe to samples was 2 cm as conducted by [17].

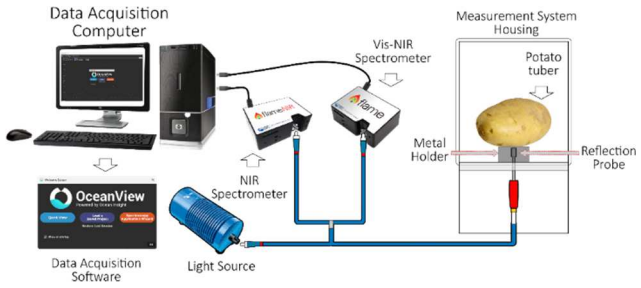

Fig. 1 Spectra measurement using modular Vis-NIR and NIR spectroscopy.

The integration time for the spectra acquisition process was set at 470 ms for Vis-NIR and 800 ms for NIR, while the average scans were 20 (Vis-NIR) and 12 (NIR), respectively. A boxcar width of 1 was employed. Calibration was executed before obtaining the sample spectra by obtaining white reference spectra using a ceramic diffuse reflectance standard (WS-1, Ocean Optics, USA) and a dark reference by deactivating the light source. Each sample was scanned ten times.

C. Sucrose Content Measurement

The sugar content of sucrose was measured for each period in the samples using a digital refractometer (HI96801, Hanna Instruments company, Woonsocket, RI), similar to the method by Costa et al. [18]. In the conventional method, potato samples blended into a fine powder were used to measure the amount of sugar. Before quantifying the sugar concentration of the specimens, the refractometer was adjusted for accuracy or calibrated by employing deionized water. The potato juice was placed on the refractometer after reaching the ambient temperature and its sugar content was measured three replicates on each sample and expressed in %.

D. Partial Least Square Regression (PLSR) Analysis

Chemometrics employs multivariate statistics to extract valuable insights from intricate analytical data. In this investigation, the utilization of partial least square regression (PLSR) was used. These models aimed to explain the structure and connections between the modular Vis–NIR spectroscopy and spectroscopic data and the corresponding chemical properties, namely sugar and acidity (pH). PLSR analysis created predictive models of sugar content (glucose, fructose, sucrose, inverted sugar) and pH. PLSR analysis is carried out by making a calibration model and testing the performance of the model. PLS calibration model creation using full cross-validation.

The reflectance spectra from Vis–NIR range (400–1000 nm) and SW–NIR range (1000–1700 nm) obtained using Ocean View 2.0.12 were collected separately and combined in Microsoft Excel®. The chemometric analyses were conducted on these spectra using Unscrambler X software version 10.4 (CAMO Software AS, Oslo, Norway). All spectra in Vis–NIR (400–1000 nm) and SW–NIR (1000–1700 nm) were combined to develop the PLSR model. The spectra were preprocessed using six different methods: standard normal variate, multiplicative scatter correction, area normalization (AN), Savitzky–Golay smoothing, Savitzky–Golay 1st derivative, and Savitzky–Golay 2nd derivative to address potential issues that could affect the accuracy of chemical composition measurement.

All spectra data were separated into calibration and prediction data sets. The evaluation of models was conducted concerning their performance of the coefficient of determination for calibration (R^2c) and root mean square error calibration (RMSEC). The root mean squared error of cross-validation (RMSECV) is used for testing calibration models by making sure they are not skewed with data points or the presence or absence of outliers. The best calibration model, according to the most effective spectral transformations indicative of the finest preprocessing spectra, was then applied to prediction data sets and the evaluation is conducted by taking into consideration the coefficient of determination of prediction (R^2p), root mean squared error of prediction (RMSEP), and RPD values.

The coefficient of determination (R^2) is used to see the relationship between two variables, namely the relationship between the actual value of the analyte and the predicted value. R^2 indicates the proportion of variability in the Y variables (sucrose data) that can be accounted for by the X variables (reflectance data). This metric effectively determines the predictive capacity of the X variables regarding the Y variables. The range of values for the coefficient of determination (R^2) is between zero (0) and one (1) and has a small Root Mean Square Error (RMSE) value. Implementing a calibration exhibiting an R2 value ranging from 0.83 to 0.90 in most use cases may be feasible, and a value above 0.92 is considered utilizable. The RMSEC and RMSEP are the square root of the mean of the squared calibration and prediction errors. It determines the error between the actual and predicted values on the calibration and prediction set.

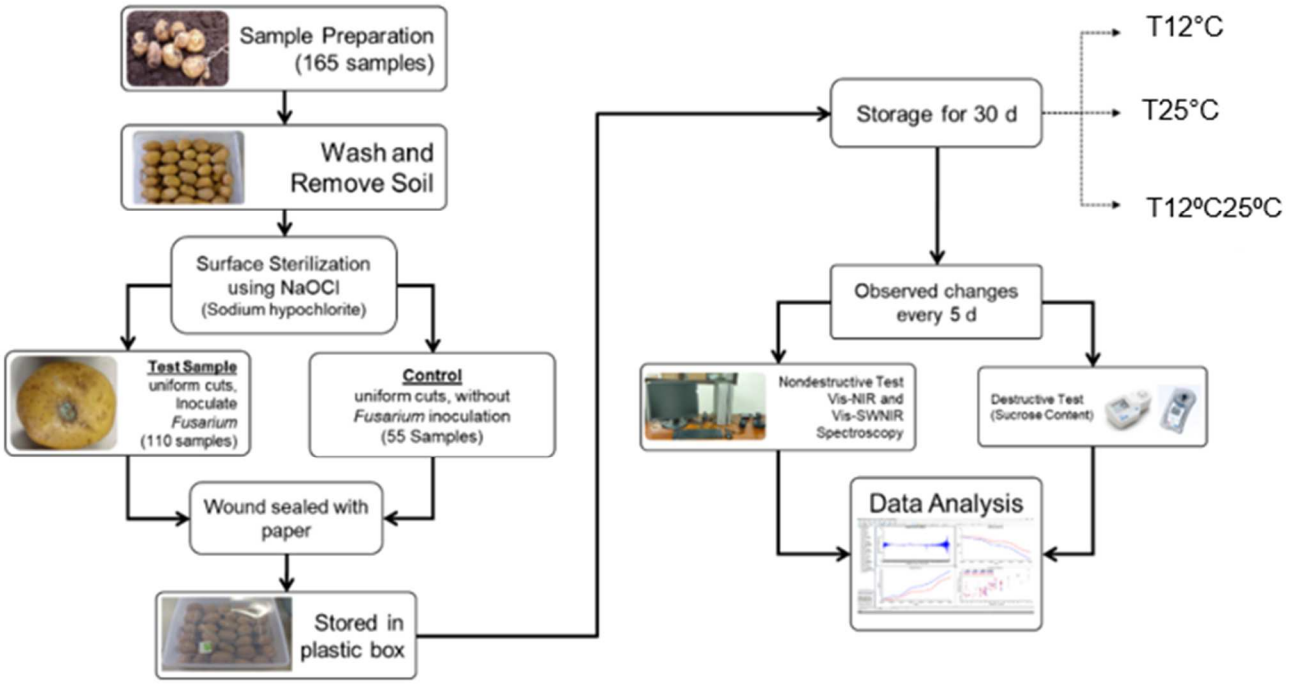

Fig. 2 The flow of research started from sample preparation, spectra measurement, and data analysis.

To assess the precision of modeling with multivariate calibration using RMSEC and RMSEP. The RPD, which stands for the ratio of the standard deviation of the reference data for the validation set to the RMSEP, is a crucial model assessment metric used to assess model effectiveness. Different ranges of RPD values, such as 1.5–2.0, 2.0–2.5, and above 2.5–3.0, can provide varying degrees of screening capabilities. These ranges correspond to rough, estimated quantitative, and excellent screening [19], [20]. An ideal model should have high R^2 and RPD values and low RMSEC and RMSEP values, with the difference between the last two values being minimal.

III. Results and Discussion

A. Sucrose Content of Potato

Table 2 shows the mean and standard deviation for sucrose content of *Granola L* potato tuber. Regardless of the storage temperature, the infected potato had higher sucrose than the noninfected potato, but the potato stored at 25°C had higher sucrose than at 12°C. According to Sim et al., non-reducing sugar content or sucrose increases in storage with temperatures below 10-12ºC. Sucrose (non-reducing sugar) content also slowly increases up to 40 days after storage, then rapidly declines during the sprouting stage [21]. According to Tiwari et al, in biotic and abiotic pressure conditions such as *Fusarium spp.* fungus infection, there is an increase in sugar content in potatoes as a marker of molecular reactions [4]. Hence, changes in chemical composition in infected potatoes tend to be faster. These findings demonstrate how temperature fluctuations affect sucrose concentrations, with significant differences between infected and noninfected samples found in all treatment groups.

TABLE II
Mean and Standard Deviation (SD) of Sucrose Content in Potato Tubers

Samples	Category	Sucrose (%) (mean ± SD)
T12°C	Noninfected (N-12)	4.95 ± 0.49
	Infected (I-12)	5.89 ± 0.42
T25°C	Noninfected (N-25)	5.04 ± 0.60
	Infected (I-25)	5.77 ± 0.64
T12ºC25ºC	Noninfected (N)	4.90 ± 0.52
	Infected (I)	6.25 ± 0.71

B. Visible and Near-Infrared (Vis/NIR) Spectra

This study uses a modular spectrometer with two probes, one for visible and near-infrared (Vis-NIR) light with wavelengths of 400-1000 nm and the other for shortwave near-infrared (SWNIR) light with wavelengths of 900-1700 nm. In Vis-NIR spectroscopy, after plotting a spectrum from 350 to 1100 nm, the wavelength ranges below 400 and above 1000 nm appeared noisy or showed interference. Therefore, for data analysis, it is expected to manually cut the spectrum only to include the wavelength range from 400 to 1000 nm [22]. Reducing noise in a spectrum aims to eliminate or decrease unwanted interference or noise, enhancing the clarity and visibility of important information in the range. According to [6], the decrease in wavelength points can speed up spectral detection, but it also reduces resolution and slightly affects the model's accuracy.

Figures 3(a), 4(a), and 5(a) show the original spectra for Noninfected (N) and infected (I) potato tubers stored at 12°C (T12°C), 25°C (T25°C), and combination storage temperatures at 12°C and 25°C (T12ºC25ºC). All spectra have a similar pattern, with an absorbance at 480 nm associated with carotenoids [23]. According to Bravo, the most essential pigments in potatoes are carotenoids, anthocyanins, and chlorophyll [24]. A lower reflectance at 670 nm suggests

chlorophyll in Noninfected (N) potatoes. This means they absorb more energy in this spectrum than infected (I) ones. Prior research reported higher chlorophyll content in healthy tomatoes than those infected with *Fusarium spp.* [14].

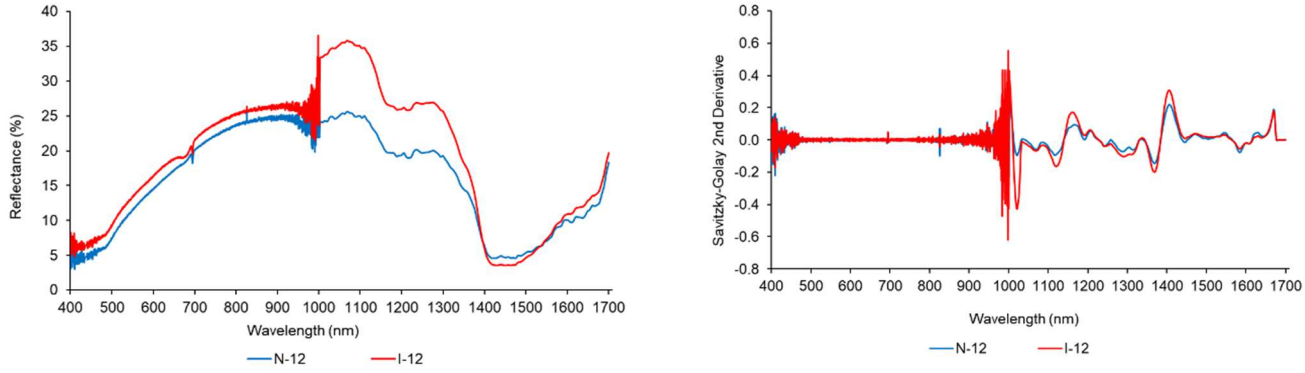

(a) (b)

Fig. 3 (a) Original spectra, and (b) Savitzky-Golay 2nd derivative (SGD2) spectra of potato tuber samples stored at 12°C (T12ºC)

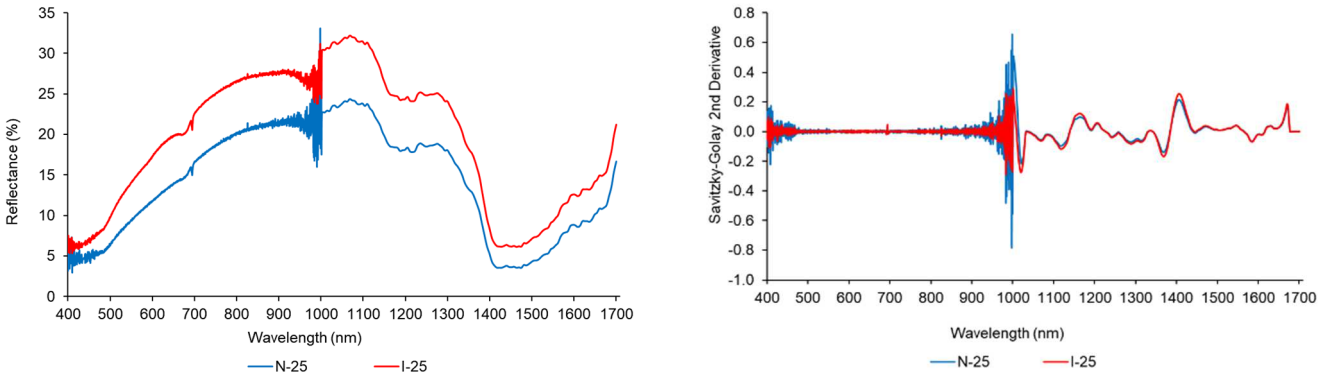

(a) (b)

Fig. 1 (a) Original spectra, and (b) Savitzky-Golay 2nd derivative (SGD2) spectra of potato tuber samples stored at 25°C (T25ºC)

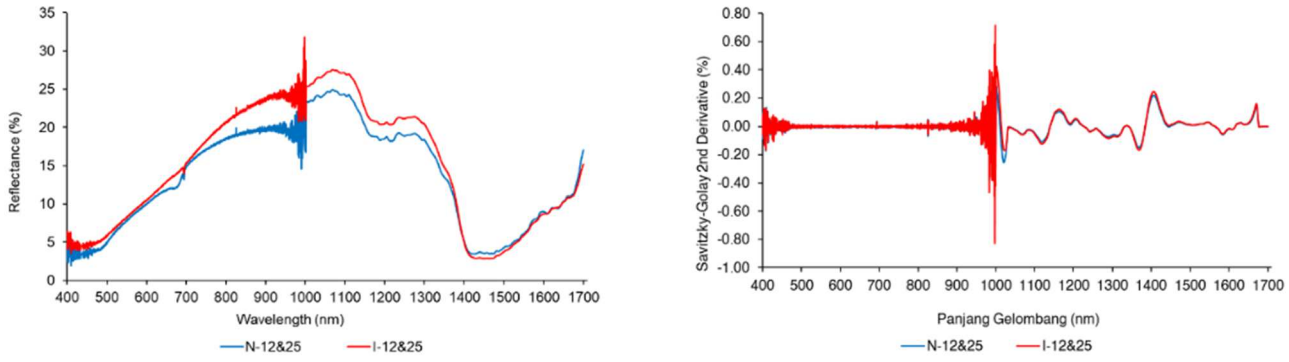

(a) (b)

Fig. 2 (a) Original spectra, and (b) Savitzky-Golay 2nd derivative (SGD2) spectra of potato tuber samples stored at 12°C and 25°C (T12ºC25ºC)

The reflectance spectra of Noninfected (N) and infected (I) potatoes showed a similar pattern. i.e., high at 900 nm, decreased to 1400 nm, and then increased to 1700 nm. The water content in the samples caused significant absorbance peaks at 995 nm, 1210 nm, and 1435 nm [12]. The absorbance of Noninfected (N) potatoes was higher than that of infected (I) potatoes at 990 nm and 1210 nm, which could be attributed to their higher water content.

Figures 3(b), 4(b), and 5(b) show the Savitzky-Golay 2nd derivative (SGD2) spectra for Noninfected (N) and infected (I) potato tubers stored at 12°C (T12°C), 25°C (T25°C), and combination storage temperatures at 12°C and 25°C (T12ºC25ºC). It was shown that the SDG2 enhanced spectral resolution and revealed critical information about potato parameters, such as sugar content and pH. Infected (I) and Noninfected (N) potatoes show significant variation in absorbance between 400 - 700 nm and 700 - 950 nm. High reflectance at 690 nm in potato spectra correlates with chlorophyll, while 770 nm correlates with fructose and glucose [25]. A significant increase in peak absorption resolution between 1065 and 1335 nm represents the sugar content of glucose and fructose) [26]. Other absorption peaks or reflectance are seen at wavelengths of 1370 nm. SW-NIR bands in the 1355-1400 nm region, seen in all three potato spectra with different storage temperature treatments,

represent the second overtone of the C-H combination (carbohydrates, fats) [27].

C. PLSR Model

The PLSR calibration model was developed using calibration datasets to predict the sucrose content of potatoes under different storage conditions. Table 3 shows the calibration and prediction datasets used in constructing the Partial Least Squares Regression (PLSR) model for predicting sucrose content (%) across multiple sample categories and temperature conditions. In general, Table 3 shows that datasets for calibration and prediction had similar values.

TABLE II
CALIBRATION AND PREDICTION DATASETS WERE USED IN DEVELOPING THE PLSR MODEL FOR PREDICTING SUCROSE CONTENT.

Samples		Category	Sucrose (%) (mean ± SD)
Calibration	T12°C	Noninfected (N-12)	4.93 ± 0.49
		Infected (I-12)	5.88 ± 0.42
	T25°C	Noninfected (N-25)	5.04 ± 0.60
		Infected (I-25)	5.79 ± 0.63
	T12ºC25ºC	Noninfected (N-P)	4.89 ± 0.51
		Infected (I-P)	6.27 ± 0.70
Prediction	T12°C	Noninfected (N-12)	4.98 ± 0.50
		Infected (I-12)	5.91 ± 0.42
	T25°C	Noninfected (N-25)	5.06 ± 0.62
		Infected (I-25)	5.74 ± 0.66
	T12ºC25ºC	Noninfected (N-P)	4.90 ± 0.55
		Infected (I-P)	6.23 ± 0.74

Table 4 shows the PLSR results for sucrose prediction using a combination of Vis-NIR and SWNIR wavelengths of 400 – 1700 nm. The results for RMSEC, RMSEP, and RPD differed depending on the preprocessing method and temperature. The best calibration model for predicting sucrose in healthy and *Fusarium spp*-infected potatoes was achieved using Savitzky-Golay 1st or 2nd Derivative. Potato stored at 25ºC and a combination of 12ºC and 25ºC resulted in higher R^2c than the lower temperature of 12 ºC. The best PLSR models produced lower RMSEC and RMSEP values, suggesting increased model correctness, and obtained higher RPD values, showing improved prediction reliability. These findings highlight the need to use proper preprocessing approaches to enhance the performance of PLSR models for predicting sucrose concentration in potato tubers under varied temperature settings.

TABLE III
THE RESULTS OF CALIBRATION AND PREDICTION OF SUCROSE CONTENT OF POTATO TUBER BY USING PLSR WITH SEVERAL PREPROCESSING METHODS

		Preprocessing methods						
		RAW	**AN**	**SNV**	**MSC**	**SGS**	**1st SGD**	**2nd SGD**
T12°C	R^2c	0.54	0.01	0.59	0.00	0.49	0.64	0.65
	RMSEC	0.44	0.65	0.42	0.65	0.47	0.39	0.39
	R^2p	0.55	0.01	0.49	0.00	0.46	0.60	0.67
	RMSEP	0.44	0.65	0.48	0.65	0.48	0.41	0.38
	RPD	1.48	1.00	1.37	1.00	1.35	1.58	1.73
T25°C	R^2c	0.61	0.76	0.74	0.80	0.55	0.87	0.84
	RMSEC	0.45	0.35	0.36	0.32	0.48	0.26	0.29
	R^2p	0.62	0.45	0.44	0.04	0.40	0.75	0.72
	RMSEP	0.44	0.55	0.54	1.68	0.56	0.36	0.38
	RPD	1.63	1.30	1.32	0.43	1.28	1.99	1.89
T12ºC25ºC	R^2c	0.72	0.76	0.80	0.81	0.64	0.77	0.83
	RMSEC	0.37	0.33	0.31	0.30	0.41	0.33	0.28
	R^2p	0.57	0.68	0.62	0.67	0.53	0.75	0.78
	RMSEP	0.46	0.39	0.45	0.41	0.48	0.35	0.32
	RPD	1.96	2.29	2.01	2.18	1.87	2.56	2.81

The calibration model employing PLSR for quantifying sucrose content in potatoes stored at a temperature of 12°C exhibited a relatively low R^2c value of 0.65 and RMSEC of 0.39 using the Savitzky-Golay 2nd Derivative spectra. This model was able to predict the sucrose content with R2p accurately of 0.67, RMSEP of 0.38, and RPD of 1.73. However, although the RPD value meets the requirements for a predictive model, the R2 is not feasible because it is less than 0.82.

The Savitzky-Golay 1st Derivative method was applied to the original spectra to quantify the sucrose content in potato tubers stored at 25°C resulted in a higher R^2c of 0.87 and a lower RMSEC of 0.26. The model could predict the sucrose content with R^2p of 0.75, RMSEP of 0.36, and RPD of 1.99. The Savitzky-Golay 2nd Derivative method was applied to the original spectra to quantify sucrose content in potatoes stored at 12°C and 25°C temperatures, resulting in R^2c of 0.83 and RMSEC of 0.28. Based on this approach, the model could predict the sucrose content with R^2p of 0.78, RMSEP of 0.32, and RPD of 2.14.

The statistical values obtained from the experimental data were within an acceptable range, suggesting that the mathematical models used to quantify the sucrose levels in this investigation were satisfactory and suitable for potential implementation in agriculture [28]. In other studies, R^2 values of 0.81 were obtained for sucrose in potato tuber stored at 12°C temperature [29], R^2 values of 0.78 were obtained for sucrose in mandarin fruit [30], and R^2 values of 0.92 were obtained for sucrose in molasses stored at 25°C [31].

The PLS loadings or regression coefficient analysis (known as β-coefficient) was used to denote which wavelengths are essential in a given PLSR of the sucrose content model [32]. The regression coefficients for the prediction of sugar content, specifically sucrose on potato storage at 12°C using the Savitzky-Golay 2nd Derivative method is illustrated in Figure 6. In the Vis-NIR wavelength range, some of the most prominent peaks in potato spectra are absorbance at 407 nm and 925 – 975 nm. Peak absorbance at 407 nm is likely correlated with carotenoids [33]. Peak absorbance at 925 – 975 nm is likely correlated with the third overtone of the C-H stretch, the first overtone of O-H, the combination of the O-H stretch, and the deformation mode of sucrose. According to Rongtong et al., the PLSR model for estimating sucrose content in papaya was obtained in the wavelength range of 910 – 1162 nm and 1350 – 1792 nm and produced R^2C value of 0.97 [34]. The wavelength range identified at 1008 – 1631 nm is likely correlated with the second overtone combinations of CH or OH in sucrose [35]. In the NIR wavelength range of the potato storage spectra at 12°C, reflectance at 1432 nm (adjacent to 1440 nm) correlates with the first overtone O–H stretch of sucrose and starch structures.

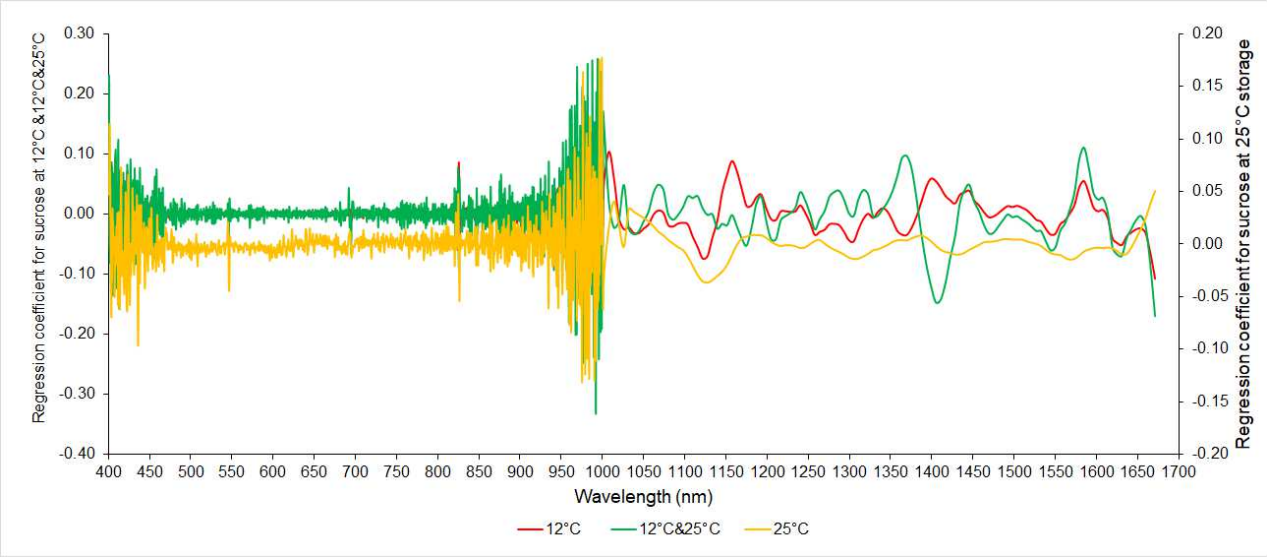

Fig. 3 The regression coefficient of PLSR using the Savitzky-Golay 2nd Derivative method for quantification of sucrose content in potato storage at 12°C and a combination of 12°C and 25°C and the Savitzky-Golay 1st Derivative method at 25°C storage temperature.

Figure 6 shows that potato spectra at storage temperatures of 12°C using the Savitzky-Golay 2nd Derivative method and 25°C using the Savitzky-Golay 1st Derivative method in the Vis-NIR wavelength region (400 – 1000 nm) exhibit similar absorbance at 407 nm and 925 – 975 nm. However, they differ in the lower absorbance at 825 nm and 888 nm. The apparent absorption at 550 nm may correlate with the chlorophyll content in potatoes [36], [37]. As the severity of disease infection increases, the chlorophyll content in potatoes decreases, leading to a weaker reflection of green light and damage to the leaf cell wall—consequently, the reflection at 550 nm and the NIR spectral band decrease.

Potato spectra obtained during pretreatment, which involves storage at combination temperatures of 12°C and 25°C, exhibited absorption peaks at the following wavelengths: 400 – 500 nm, 545 nm, 695 nm, 825 nm, 925 – 975 nm, 1038 nm, 1175 nm, 1210 nm, 1405 nm, 1544 nm, and 1631 nm. Reflectance peaks were also observed at wavelengths of 1364 nm, 1445 nm, and 1585 nm. Wavelengths in the 400 – 500 nm range are likely associated with high carotenoid content in potatoes [38]. Carotenoids are natural pigments responsible for many fruits and vegetables' yellow, orange, and red colors [39]. While potato skin color typically ranges from brown to creme, the flesh is usually white or light.

IV. Conclusion

The results indicate that Vis-NIR can replace conventional methods, allowing for fast, simple, and safe processing of multiple parameters. The Vis-NIR technology's ability to accurately predict the sugar content and pH of potatoes stored at 12°C was low and categorized as sufficient performance.

The sucrose calibration models for potato storage at 12°C show R^2c and RMSEC of 0.65 and 0.39, respectively. When applied to predict sucrose content, the models result in R^2p of 0.65, RMSEP of 0.38, and RPD of 1.73. However, the Vis-NIR models developed in this study showed some relevance in providing rough estimates of the sugar content of potatoes stored at 25°C and during pretreatment or combined temperature storage (12°C and 25°C). The calibration models for potato storage at 25°C and a combination of 12°C and 25°C show R^2c of 0.87 and 0.83 and RMSEC of 0.26 and 0.28, respectively. When applied to predict the sugar content and pH of potatoes stored at ±25°C and during pretreatment, the models resulted in R^2p of 0.75 and 0.78, RMSEP of 0.36 and 0.32, and RPD of 1.99 and 2.81 for sucrose. The RPD value shows the result of sufficient and good performance. These estimates can be helpful for qualitatively sorting potato batches that exceed the acceptable upper limit for sugar content, thus helping to identify healthy potatoes. Further investigation and validation are essential to develop robust and dependable models for Vis-NIR spectroscopy in potato processing. This should be coupled with a deeper understanding of potato types and storage environment variations. Developing a modular Vis-NIR spectrometer with a system to choose the most suitable predictive model would facilitate on-site material detection and ultimately lead to a more adaptable apparatus for the potato processing industry.

ACKNOWLEDGMENT

The authors thank PT. BISI International, Tbk (Seed and Agrochemical Company, Indonesia) for the support.

CONFLICT OF INTEREST

The authors declare that they have no known competing conflict of interest that could have appeared to influence the work reported in this paper.

REFERENCES

[1] S. Wang, H. Tian, S. Tian, J. Yan, Z. Wang, and H. Xu, "Evaluation of dry matter content in intact potatoes using different optical sensing modes," *J. Food Meas. Charact.*, vol. 17, no. 3, pp. 2119–2134, 2023, doi: 10.1007/s11694-022-01780-w.

[2] W. Food, *World Food and Agriculture – Statistical Yearbook 2022*. 2022. doi: 10.4060/cc2211en.

[3] R. R. P. da Conceição *et al.*, "Application of near-infrared hyperspectral (NIR) images combined with multivariate image analysis in the differentiation of two mycotoxicogenic Fusarium species associated with maize," *Food Chem.*, vol. 344, no. November 2020, 2021, doi: 10.1016/j.foodchem.2020.128615.

[4] R. K. Tiwari *et al.*, "Impact of Fusarium dry rot on physicochemical attributes of potato tubers during postharvest storage," *Postharvest Biol. Technol.*, vol. 181, no. July, p. 111638, 2021, doi:10.1016/j.postharvbio.2021.111638.

[5] Q. Hu *et al.*, "Potatoes dormancy release and sprouting commencement: A review on current and prospects," *Food Front.*, vol. 4, no. 3, pp. 1001–1018, 2023, doi: 10.1002/fft2.228.

[6] M. Han *et al.*, "Variable selection for the determination of the soluble solid content of potatoes with surface impurities in the visible/near-infrared range," *Biosyst. Eng.*, vol. 209, pp. 170–179, Sep. 2021, doi:10.1016/j.biosystemseng.2021.06.019.

[7] M. W. Haider *et al.*, "Postharvest dormancy-related changes of endogenous hormones in relation to different dormancy-breaking methods of potato (Solanum tuberosum L.) tubers," *Front. Plant Sci.*, vol. 13, 2022, doi: 10.3389/fpls.2022.945256.

[8] R. K. Tiwari *et al.*, "Impact of Fusarium Infection on Potato Quality, Starch Digestibility, In Vitro Glycemic Response, and Resistant Starch Content," *J. Fungi*, vol. 9, no. 4, 2023, doi: 10.3390/jof9040466.

[9] G. Bedini, S. S. N. Chakravartula, M. Nardella, A. Bandiera, R. Massantini, and R. Moscetti, "Prediction of potato dry matter content by FT-NIR spectroscopy: Impact of tuber tissue on model performance," *Futur. Foods*, vol. 8, no. September 2022, p. 100241, 2023, doi: 10.1016/j.fufo.2023.100241.

[10] S. V. Gudkov *et al.*, "Optical Methods for the Detection of Plant Pathogens and Diseases (Review)," *AgriEngineering*, vol. 5, no. 4, pp. 1789–1812, Oct. 2023, doi: 10.3390/agriengineering5040110.

[11] M. E. Raypah, L. J. Zhi, L. Z. Loon, and A. F. Omar, "Near-infrared spectroscopy with chemometrics for identification and quantification of adulteration in high-quality stingless bee honey," *Chemom. Intell. Lab. Syst.*, vol. 224, no. February, p. 104540, 2022, doi:10.1016/j.chemolab.2022.104540.

[12] A. Rady, D. E. Guyer, W. Kirk, and I. Donis-González, "Prediction of the Leaf Primordia of Potato Tubers Using Sensor Fusion and Wavelength Selection," *J. Imaging*, vol. 5, p. null, 2019, doi:10.1117/12.2621682.

[13] B. Nieto-Ortega, J. J. Arroyo, C. Walk, N. Castañares, E. Canet, and A. Smith, "Near infrared reflectance spectroscopy as a tool to predict non-starch polysaccharide composition and starch digestibility profiles in common monogastric cereal feed ingredients," *Anim. Feed Sci. Technol.*, vol. 285, no. May 2021, 2022, doi:10.1016/j.anifeedsci.2022.115214.

[14] M. S. Attia, D. A. El-Wakil, A. H. Hashem, and A. M. Abdelaziz, "Antagonistic Effect of Plant Growth-Promoting Fungi Against Fusarium Wilt Disease in Tomato: In vitro and In vivo Study," *Appl. Biochem. Biotechnol.*, vol. 194, no. 11, pp. 5100–5118, 2022, doi:10.1007/s12010-022-03975-9.

[15] L. Cui, X. Wang, Y. Xu, Y. Li, and M. Han, "Hyperspectral reflectance imaging for water content and firmness prediction of potatoes by optimum wavelengths," *J. Consum. Prot. Food Saf.*, vol. 17, no. 1, pp. 51–64, Mar. 2022, doi: 10.1007/s00003-021-01343-z.

[16] S. Farokhzad, A. Modaress Motlagh, P. Ahmadi Moghaddam, S. Jalali Honarmand, and K. Kheiralipour, "A machine learning system to identify progress level of dry rot disease in potato tuber based on digital thermal image processing," *Sci. Rep.*, vol. 14, no. 1, pp. 1–10, 2024, doi: 10.1038/s41598-023-50948-x.

[17] M. F. R. Pahlawan, R. K. Wati, and R. E. Masithoh, "Development of a low-cost modular VIS/NIR spectroscopy for predicting soluble solid content of banana," in *IOP Conference Series: Earth and Environmental Science*, 2021, vol. 644, no. 1. doi: 10.1088/1755-1315/644/1/012047.

[18] V. Gomes, M. S. Reis, F. Rovira-Más, A. Mendes-Ferreira, and P. Melo-Pinto, "Prediction of sugar content in port wine vintage grapes using machine learning and hyperspectral imaging," *Processes*, vol. 9, no. 7, 2021, doi: 10.3390/pr9071241.

[19] A. A. Munawar, Zulfahrizal, H. Meilina, and E. Pawelzik, "Near infrared spectroscopy as a fast and non-destructive technique for total acidity prediction of intact mango: Comparison among regression approaches," *Comput. Electron. Agric.*, vol. 193, no. 3, p. 106657, 2022, doi: 10.1016/j.compag.2021.106657.

[20] M. D. C. García-García *et al.*, "Determination of Quality Parameters in Mangetout (Pisum sativum L. ssp. arvense) by Using Vis/Near-Infrared Reflectance Spectroscopy," *Sensors*, vol. 22, no. 11, Jun. 2022, doi: 10.3390/s22114113.

[21] E. Sim, J. Kim, H. S. Kim, H. Y. Park, and H. S. Choi, "Physicochemical characteristics of three potato cultivars grown in different cultivation periods," *J. Food Compos. Anal.*, vol. 119, no. November 2022, p. 105215, 2023, doi: 10.1016/j.jfca.2023.105215.

[22] Y. Yang, Z. Liu, M. Huang, Q. Zhu, and X. Zhao, "Automatic detection of multi-type defects on potatoes using multispectral imaging combined with a deep learning model," *J. Food Eng.*, vol. 336, no. July 2022, p. 111213, 2023, doi:10.1016/j.jfoodeng.2022.111213.

[23] D. B. Rodriguez-Amaya, "Natural food pigments and colorants," *Curr. Opin. Food Sci.*, vol. 7, pp. 20–26, 2016, doi:10.1016/j.cofs.2015.08.004.

[24] C. Bravo *et al.*, "Stability of Phenolic Compounds, Antioxidant Activity and Color Parameters in Colored-Flesh Potato Chips," *Molecules*, vol. 28, no. 16, 2023, doi: 10.3390/molecules28166047.

[25] F. Wang, C. Wang, S. Song, S. Xie, and F. Kang, "Study on starch content detection and visualization of potato based on hyperspectral imaging," *Food Sci. Nutr.*, vol. 9, no. 8, pp. 4420–4430, 2021, doi:10.1002/fsn3.2415.

[26] H. J. He, Y. Wang, M. Zhang, Y. Wang, X. Ou, and J. Guo, "Rapid determination of reducing sugar content in sweet potatoes using NIR spectra," *J. Food Compos. Anal.*, vol. 111, no. December 2021, p.

104641, 2022, doi: 10.1016/j.jfca.2022.104641.
[27] K. B. Beć, J. Grabska, and C. W. Huck, "Miniaturized NIR Spectroscopy in Food Analysis and Quality Control: Promises, Challenges, and Perspectives," *Foods*, vol. 11, no. 10, 2022.
[28] B. M. Nicolai *et al.*, "Nondestructive measurement of fruit and vegetable quality by means of NIR spectroscopy : A review," *Postharvest Biol. Technol.*, vol. 46, pp. 99–118, 2007, doi:10.1016/j.postharvbio.2007.06.024.
[29] N. U. Haase, "Prediction of potato processing quality by near infrared reflectance spectroscopy of ground raw tubers," *J. Near Infrared Spectrosc.*, vol. 19, no. 1, pp. 37–45, 2011, doi: 10.1255/jnirs.919.
[30] L. S. Magwaza *et al.*, "Assessment of rind quality of 'Nules Clementine' mandarin fruit during postharvest storage: 2. Robust Vis/NIRS PLS models for prediction of physico-chemical attributes," *Sci. Hortic. (Amsterdam).*, vol. 165, pp. 421–432, 2014, doi:10.1016/j.scienta.2013.09.050.
[31] A. Phuphaphud, K. Saengprachatanarug, J. Posom, E. Taira, and L. Panduangnate, "Prediction and Classification of Energy Content in Growing Cane Stalks for Breeding Programmes Using Visible and Shortwave Near Infrared," *Sugar Tech*, vol. 24, no. 5, pp. 1497–1509, 2022, doi: 10.1007/s12355-021-01075-2.
[32] D. Saputro, D. Priambodo, M. Pahlawan, and R. Masithoh, "Classification of Cocoa Beans Based on Fermentation Level Using PLS-DA Combined with Visible Near-Infrared (VIS-NIR) Spectroscopy," *Proc. 2nd Int. Conf. Smart Innov. Agric. (ICoSIA 2021)*, vol. 19, no. ICoSIA 2021, pp. 100–106, 2022, doi:10.2991/absr.k.220305.015.
[33] D. N. Rahmia, E. Z. D. Pratiwi, M. F. R. Pahlawan, H. Z. Amanah, and R. E. Masithoh, "Non-destructive measurement of malic acid content of sapodilla fruit using visible near infrared (VisNIR) spectroscopy with variations in storage temperature," *IOP Conf. Ser. Earth Environ. Sci.*, vol. 1116, no. 1, p. 012027, Dec. 2022, doi: 10.1088/1755-1315/1116/1/012027.
[34] B. Rongtong, T. Suwonsichon, P. Ritthiruangdej, and S. Kasemsumran, "Determination of water activity, total soluble solids and moisture, sucrose, glucose and fructose contents in osmotically dehydrated papaya using near-infrared spectroscopy," *Agric. Nat. Resour.*, vol. 52, no. 6, pp. 557–564, 2018, doi:10.1016/j.anres.2018.11.023.
[35] R. E. Masithoh, F. Roosmayanti, K. Rismiwandira, and M. F. R. Pahlawan, "Detection of Palm Sugar Adulteration by Fourier Transform Near-Infrared (FT-NIR) and Fourier Transform Infrared (FT-IR) Spectroscopy," *Sugar Tech*, no. Livesey 2003, 2021, doi:10.1007/s12355-021-01058-3.
[36] B. Hou, Y. Hu, P. Zhang, and L. Hou, "Potato Late Blight Severity and Epidemic Period Prediction Based on Vis/NIR Spectroscopy," *Agric.*, vol. 12, no. 7, 2022, doi: 10.3390/agriculture12070897.
[37] D. S. Kasampalis, P. Tsouvaltzis, K. Ntouros, A. Gertsis, D. Moshou, and A. S. Siomos, "Rapid nondestructive postharvest potato freshness and cultivar discrimination assessment," *Appl. Sci.*, vol. 11, no. 6, Mar. 2021, doi: 10.3390/app11062630.
[38] M. Šulc, Z. Kotíková, L. Paznocht, and J. Lachman, "Changes in Carotenoid Profile during Potato (Solanum tuberosum L.) Tuber Maturation," *Am. J. Potato Res.*, vol. 98, no. 2, pp. 85–92, 2021, doi:10.1007/s12230-020-09805-0.
[39] L. M. Londoño-Giraldo, A. M. Baena-Pedroza, F. Martinez-Seidel, E. Corpas-Iguarán, and G. Taborda-Ocampo, "Gone wild: Integration of antioxidative, physicochemical, volatilomic and sensorial profiles ratify rustic relatives of cherry tomato as ideal mating partners," *Sci. Hortic. (Amsterdam).*, vol. 277, no. October 2020, 2021, doi:10.1016/j.scienta.2020.109814.